Scripta Materialia xxx (2017) xxx–xxx

Contents lists available at ScienceDirect

Scripta Materialia

journal homepage: www.elsevier.com/locate/scriptamat

Viewpoint Set

Searching the weakest link: Demagnetizing fields and magnetization reversal in permanent magnets

J. Fischbacher [a], A. Kovacs [a], L. Exl [b,c], J. Kühnel [d], E. Mehofer [d], H. Sepehri-Amin [e], T. Ohkubo [e], K. Hono [e,1], T. Schrefl [a,*]

[a] Center for Integrated Sensor Systems, Danube University Krems, 2700 Wiener Neustadt, Austria
[b] Faculty of Physics, University of Vienna, 1090 Vienna, Austria
[c] Faculty of Mathematics, University of Vienna, 1090 Vienna, Austria
[d] Faculty of Computer Science, University of Vienna, 1090 Vienna, Austria
[e] Elements Strategy Initiative Center for Magnetic Materials, National Institute for Materials Science, Tsukuba 305-0047, Japan

ARTICLE INFO

Article history:
Received 1 October 2017
Received in revised form 12 November 2017
Accepted 13 November 2017
Available online xxxx

Keywords:
Permanent magnet
Micromagnetism
Grain boundary diffusion

ABSTRACT

Magnetization reversal in permanent magnets occurs by the nucleation and expansion of reversed domains. Micromagnetic theory offers the possibility to localize the spots within the complex structure of the magnet where magnetization reversal starts. We compute maps of the local nucleation field in a $Nd_2Fe_{14}B$ permanent magnet using a model order reduction approach. Considering thermal fluctuations in numerical micromagnetics we can also quantify the reduction of the coercive field due to thermal activation. However, the major reduction of the coercive field is caused by the soft magnetic grain boundary phases and misorientation if there is no surface damage.

© 2017 Acta Materialia Inc. Published by Elsevier Ltd. All rights reserved.

1. Introduction

With the rise of sustainable energy production and eco-friendly transport there is an increasing demand for permanent magnets. The generator of a direct drive wind mill requires high performance magnets of 400 kg/MW power; and on average a hybrid and electric vehicle needs 1.25 kg of high-end permanent magnets [1]. Modern high-performance magnets are based on $Nd_2Fe_{14}B$. These magnets have a high energy density product which means that the magnets can be small and still create a sufficiently large magnetic field. One weak point of $Nd_2Fe_{14}B$ is the relatively low Curie temperature as compared to SmCo based magnets. As a consequence, the coercive field of $Nd_2Fe_{14}B$ drops rapidly with increasing temperature. To enhance the operating temperature of $Nd_2Fe_{14}B$ magnets heavy rare earth elements are added. The anisotropy field of $(Nd,Dy)_2Fe_{14}B$ is higher than that of $Nd_2Fe_{14}B$ and therefore the Dy containing magnet can be operated at higher temperature. Production techniques that increase the Dy concentration near the grain boundary [2,3] reduce the share of heavy rare earths. In these magnets the anisotropy field is locally enhanced near the grain boundary which suppresses the formation of reversed domains [4,5]. Similarly, an enhancement of the coercive field has been achieved by Nd—Cu grain boundary diffusion [6].

The enhancement of coercivity by modification of the region next to the grain boundaries is a clear indication that magnetization reversal in permanent magnets is induced by the nucleation of a reversed domain near the grain surface. In $Nd_2Fe_{14}B$ based permanent magnets weakly ferromagnetic grain boundary phases [7] act as nucleation sites [8] if there exist no grains with reversed magnetic domains at remanence. In addition to the presence of the soft magnetic grain boundary phase, magnetization reversal is facilitated by the local demagnetizing field. These fields obtain their highest values near the edges and corners of the polyhedral grain structure [9]. Traditionally the effect of defects where the intrinsic properties are different from the bulk and the effect of the demagnetizing field on coercivity is expressed as [10]

$$H_c(T) = \alpha H_N(T) - N_{eff} M_s(T). \quad (1)$$

Here $H_N = 2K_1/(\mu_0 M_s)$ is the ideal nucleation field. The constant μ_0 is the permeability of vacuum. The anisotropy constant and the magnetization are denoted by K_1 and M_s. H_N and M_s are intrinsic magnetic properties and depend on the composition of the magnetic phase and on the temperature T. On the other hand, the coercive field, H_c, strongly changes with the microstructure of the magnet. Therefore, many researchers refer to α and N_{eff} as microstructural parameters. The parameter α gives the reduction of the coercive field by soft magnetic defects and

* Corresponding author at: Center for Integrated Sensor Systems, Danube University Krems, Viktor Kaplan Straße 2 - Bauteil E, 2700 Wiener Neustadt, Austria.
E-mail address: thomas.schrefl@donau-uni.ac.at (T. Schrefl).

[1] Kazuhiro Hono was an editor of the journal during the review period of the article. To avoid a conflict of interest, Prof. Jeff Th.M. DeHosson acted as editor for this manuscript.

https://doi.org/10.1016/j.scriptamat.2017.11.020
1359-6462/© 2017 Acta Materialia Inc. Published by Elsevier Ltd. All rights reserved.

Please cite this article as: J. Fischbacher, et al., Searching the weakest link: Demagnetizing fields and magnetization reversal in permanent magnets, Scripta Materialia (2017), https://doi.org/10.1016/j.scriptamat.2017.11.020

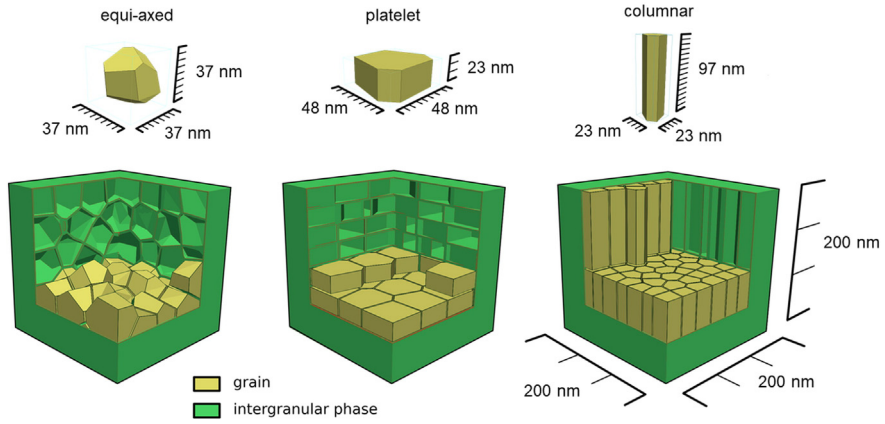

Fig. 1. Grain structures used for computing the microstructural parameters as function of the shape of the grains. The volume fraction of the grain boundary phase is 26%.

misorientation of the anisotropy axes with respect to the applied field direction; the parameter N_{eff} describes the reduction of the coercive field owing to the self-demagnetizing field. It can be regarded as a local, effective demagnetization factor.

Eq. (1) describes the influence of the microstructure on the coercive field. Temperature effects are included through the temperature dependence of $K_1(T)$, $M_s(T)$. A second mechanism how temperature influences the coercive field are thermal fluctuations on the macroscopic scale. These fluctuations may drive the system over a finite energy barrier. Hysteresis in a non-linear system like a permanent magnet results from the path formed by subsequently following local minima in an energy landscape constantly changed by a varying external field [11]. With increasing opposing field, the energy barrier that separates the system from the reversed state decreases. The critical field at which the energy barrier vanishes is the switching field of the magnet [12]. Switching at finite temperature can occur at non-zero energy barrier. If the system can escape over the energy barrier within the measurement time switching will occur. In permanent magnets it is assumed that the system can escape an energy barrier of 25 k_BT within 1 s [13]. Therefore, to include the reduction of coercivity by thermal activation Eq. (1) can be rewritten as [14,15]

$$H_c(T) = \alpha H_N(T) - N_{\text{eff}} M_s(T) - H_f(T). \tag{2}$$

The thermal fluctuation field, H_f, can be expressed in terms of the activation volume v [13]

$$H_f(T) = \frac{25\, k_B T}{\mu_0 M_s v} \tag{3}$$

Here $k_B = 1.38 \times 10^{-23}$ J/K is the Boltzmann constant. In this work we will quantify the influence of demagnetizing fields and thermal activation on the reduction of the coercive field with respect to the ideal nucleation field using micromagnetic simulations. The paper is organized as follows.

1. We will use Eq. (1) and analyze micromagnetic results for $H_c(T)$ to show how α and N_{eff} changes with the microstructure.
2. We will apply a simplified micromagnetic model based on the local demagnetizing field near the grain boundaries to get a deeper insight on how demagnetizing effects reduce coercivity.
3. We will calculate the thermally activated switching to locate the weakest spot where magnetization reversal is initiated within a complex grain structure.

For the computations of α and N_{eff} (see point (1 above) we used a finite element micromagnetic solver [16]. The hysteresis loop is computed by minimization of the Gibbs free energy for decreasing external field. The simplified micromagnetic model (see point (2 above) is based on a method for computing the demagnetizing field from surface charges [17] and a method for computing the switching field as function of field angle in the presence of defects [18]. Thermally activated switching (see point (3 above) is computed using a modified string method [19,20]. The finite element meshes are created with Tetgen [21]. At all surfaces the mesh size is 2.4 nm.

2. Results

2.1. Microstructural parameters and the demagnetizing field

We computed the coercive field for a magnet consisting of equi-axed, platelet shaped, or columnar grains. The microstructure used for the simulations is shown in Fig. 1. The grains are perfectly aligned. The edge length of the cube forming the magnet is 200 nm. The volume fraction of the grain boundary is 26%. Its thickness is 3.8 nm. For the grains we used the intrinsic magnetic properties of $Nd_2Fe_{14}B$ as function of temperature [22]. We performed two sets of simulations. In set 1 the grain boundary phase was non-magnetic; in set 2 the grain boundary phase was assumed to be weakly ferromagnetic. We set the magnetization of the grain boundary phase to 1/3 of the value for $Nd_2Fe_{14}B$, that is $M_{s,GB} = M_s/3$. The same material as in the grain boundary phase is used as surface layer with a thickness of 1.9 nm that covers the magnet. The purpose of this layer is to mimic surface damage. Please note that we change the exchange constant of all phases according to $A(T) = cM_s^2(T)$, where the factor c is determined from the $Nd_2Fe_{14}B$ values at $T = 300$ K ($\mu_0 M_s = 1.6$ T and $A = 8$ pJ/m). We apply the finite element method to compute the magnetization as function of the external field, $M(H_{\text{ext}})$. At each step of the external field the micromagnetic energy is minimized using a modified non-linear conjugate gradient method [16]. To compute the microstructural parameters, we applied the same procedure as usually done in experiments. We plotted $H_c(T)/M_s(T)$ as function of $H_N(T)/M_s(T)$ and fitted a straight line. Table 1 gives the microstructural parameters for the different structures.

Table 1
Microstructural parameters for magnets made of equi-axed, platelet shaped, and columnar grains.

Shape of grains	Grain boundary phase	α	N_{eff}
Columnar	Non-magnetic	0.88	0.79
Equi-axed	Non-magnetic	0.88	0.87
Platelet	Non-magnetic	0.88	0.91
Columnar	Weakly ferromagnetic	0.45	0.10
Equi-axed	Weakly ferromagnetic	0.47	0.27
Platelet	Weakly ferromagnetic	0.51	0.43

Please cite this article as: J. Fischbacher, et al., Searching the weakest link: Demagnetizing fields and magnetization reversal in permanent magnets, Scripta Materialia (2017), https://doi.org/10.1016/j.scriptamat.2017.11.020

Download English Version:

https://daneshyari.com/en/article/7910254

Download Persian Version:

https://daneshyari.com/article/7910254

Daneshyari.com